Nitrogen recycling in subducted mantle rocks and implications for the global nitrogen cycle

Ralf Halama[1,*], Gray E. Bebout[2], Timm John[3] and Marco Scambelluri[4]

[1] Institut für Geowissenschaften and SFB 574, Universität Kiel, Ludewig-Meyn-Str. 10, 24118 Kiel, Germany

[2] Department of Earth and Environmental Sciences, Lehigh University, 1 West Packer Avenue, Bethlehem, Pennsylvania 18015, USA

[3] Institut für Mineralogie, Universität Münster, Corrensstr. 24, 48149 Münster, Germany

[4] Dipartimento per lo Studio del Territorio e delle sue Risorse, Università di Genova, Corso Europa 26, 16132 Genova, Italy

* Corresponding author contact information:

Ralf Halama

Institut für Geowissenschaften and SFB 574

Universität Kiel, 24098 Kiel, Germany

E-mail: rh@min.uni-kiel.de Tel: +49-431-880-1911 Fax: +49-431-880-4457

Abstract

The nitrogen concentrations [N] and isotopic compositions of ultramafic mantle rocks that represent various dehydration stages and metamorphic conditions during the subduction cycle were investigated to assess the role of such rocks in deep-Earth N cycling. The samples analyzed record low-grade serpentinization on the seafloor and/or in the fore-arc wedge (low-grade serpentinites from Monte Nero/Italy and Erro Tobbio/Italy) and two successive stages of metamorphic dehydration at increasing pressures and temperatures (high-pressure (HP) serpentinites from Erro Tobbio/Italy and chlorite harzburgites from Cerro del Almirez/Spain) to allow for the determination of dehydration effects in ultramafic rocks on the N budget.

In low-grade serpentinites, $\delta^{15}N_{air}$ values (-3.8 to +3.5‰) and [N] (1.3-4.5 μg/g) are elevated compared to the pristine depleted MORB mantle ($\delta^{15}N_{air}$ ~ -5‰, [N] = 0.27±0.16 μg/g), indicating input from organic-sedimentary sources, at the outer rise during slab bending and/or in the forearc mantle wedge during hydration by slab-derived fluids. Both HP serpentinites and chlorite harzburgites have $\delta^{15}N_{air}$ values and [N] overlapping with low-grade serpentinites, indicating no significant loss of N during metamorphic dehydration and retention of N to depths of 60-70 km. The best estimate for the $\delta^{15}N_{air}$ of ultramafic rocks recycled into the mantle is +3±2‰. The global N subduction input flux in serpentinized oceanic mantle rocks was calculated as 2.3 x 10^8 mol N_2/year, assuming a thickness of serpentinized slab mantle of 500 m. This is at least one order of magnitude smaller than the N fluxes calculated for sediments and altered oceanic crust. Calculated global input fluxes for a range of representative subducting sections of unmetamorphosed and HP-metamorphosed slabs, all incorporating serpentinized slab mantle, range from 1.1 x 10^{10} to 3.9 x 10^{10} mol N_2/year. The best estimate for the $\delta^{15}N_{air}$ of the subducting slab is +4±1‰, supporting models that invoke recycling of subducted N in mantle plumes and consistent with general models for the volatile evolution on Earth. Estimates of the efficiency of arc return of subducted N are

complicated further by the possibility that mantle wedge hydrated in forearcs, then dragged to beneath volcanic fronts, is capable of conveying significant amounts of N to subarc depths.

1. INTRODUCTION

Knowledge of the amount of N being subducted and the extent to which N is released from subducting rocks during devolatilization is of fundamental importance in understanding Earth's nitrogen (N) cycle and the evolution of volatile elements throughout Earth's history. Significant differences in the N isotopic composition of Earth's major reservoirs make N isotopes a useful tracer of crustal and volatile recycling. Estimates of the amounts and isotopic compositions of subducted N are critical in evaluating whether or not the N isotope compositions of certain mantle-derived magmas reflect retention of N in deeply subducted oceanic lithosphere and sediments (Marty and Dauphas, 2003; Jia et al., 2003). It is also critical in attempts to balance subduction zone N inputs from the subducting plate with N outputs in arc volcanic gases (Elkins et al., 2006; Li et al., 2007; Mitchell et al., 2010). For N, the presence of a significant imbalance between a large, isotopically heavy subducted flux compared to an isotopically light, relatively small outgassed flux suggests that significant amounts of N were trapped in the mantle during Earth's history (Javoy, 1997; 1998).

Nitrogen in the Earth's mantle as sampled by diamonds and MORB is depleted relative to the atmosphere in the heavy isotope ^{15}N ($\delta^{15}N$ ~ -5‰, where $\delta^{15}N = [(^{15}N/^{14}N)_{sample}/(^{15}N/^{14}N)_{air}-1]\bullet1000$) (Cartigny et al., 1998; Marty and Dauphas, 2003). In contrast, N in sedimentary rocks is generally enriched in ^{15}N, with $\delta^{15}N$ values for modern sediment mostly in the range of 0 to +10‰ (Kerrich et al., 2006). Because the abundance of N in the lithosphere is largely tied to its fixation by organic processes in sedimentary environments, N is a sensitive tracer of sediment-derived fluids (Bebout, 1997). Despite lower

N concentrations than in sediments, altered oceanic crust (AOC) is also an important contributor to the subduction zone nitrogen budget due to its comparatively large volume (Li et al., 2007; Mitchell et al., 2010). On the other hand, little is known about the role of the slab mantle section (Philippot et al., 2007; Halama et al., 2010). Whereas the N content in the unmodified mantle is much lower than in sediment or AOC, the effects of seafloor alteration and serpentinization could potentially lead to an increase in N concentration and the incorporation of isotopically heavier N, as observed for seafloor-altered oceanic crust, caused by the addition of sedimentary-organic N from pore fluids (Busigny et al., 2005; Li et al., 2007). Moreover, the volume of hydrated slab mantle being subducted is potentially greater than that of crust and sediment. It has previously been demonstrated that the slab mantle can convey significant amounts of H_2O (Rüpke et al., 2004) and a variety of trace elements (Scambelluri et al., 1997; 2004), including halogens (John et al., 2011), to great depths in subduction zones. The magnitude of N subduction in hydrated slab mantle must be evaluated to better constrain the degree to which N is retained in subducting slabs or returned to the atmosphere or various forearc reservoirs.

There has been considerable debate regarding whether initially subducted N largely enters the deep mantle beyond subarc depths or whether it is returned via forearc devolatilization or arc volcanism (Sano et al., 2001; Hilton et al., 2002; Fischer et al., 2002; Snyder et al., 2003; Busigny et al., 2003; Li and Bebout, 2005). Recent studies of the volcanic arc return of subducting N in the Central America and Izu-Bonin-Mariana margins, taking into account N subduction in sediment and AOC, demonstrate that a large proportion of the N entering these trenches is either lost in forearcs or delivered to the deep mantle beyond sub-arc depths (Elkins et al., 2006; Mitchell et al., 2010; Sadofsky and Bebout, 2003). For the Izu-Bonin-Mariana margin, Mitchell et al. (2010) estimated that only 4-17% of the N being subducted in sediments and AOC (total subduction input of 6.65×10^8 mol N_2/year) is being returned via arc volcanism (0.25 to 1.11×10^8 mol N_2/year, calculated by three different methods). Taking into account the additional N input flux in subducted oceanic lithospheric mantle, which depends on the degree of N enrichment by serpentinization, would create an even greater imbalance between the subduction inputs and the arc volcanic outputs. Yet another possibility is that parts of the forearc mantle wedge are hydrated and enriched in slab-derived N, then dragged to beneath volcanic fronts, potentially conveying significant amounts of N to subarc depths. This mechanism of down-dragging and deeper dehydration of forearc serpentinite has been invoked in a number of geochemical studies of arc lavas (e.g., Tatsumi and Kogiso, 1997; Straub and Layne, 2003; Tonarini et al., 2007; Johnson et al., 2009) and of serpentinized peridotites from forearc serpentine seamounts (Savov et al., 2005; 2007).

Several studies of metasedimentary rocks have evaluated whether there is significant loss of isotopically fractionated N during prograde metamorphic dehydration in forearcs. Based on study of low-grade units of the Catalina Schist and a traverse of HP/UHP metasedimentary rocks in the Italian Alps, it appears that along relatively cool prograde metamorphic P-T paths such as those experienced in most modern-Earth subduction zones, sedimentary N is largely retained during forearc metamorphism to depths beneath arcs (Bebout and Fogel, 1992; Busigny et al., 2003). In contrast, increased $\delta^{15}N$ values and decreased N concentrations with increasing metamorphic grade, interpreted as the result of preferential loss of ^{14}N to the fluid phase, occur in subducting sediments that experienced higher-T prograde metamorphic paths (Bebout and Fogel, 1992; Haendel et al., 1986; Mingram and Bräuer, 2001). In metamorphosed basaltic rocks, N concentrations and $\delta^{15}N$ overlapping with those of AOC indicate negligible effects of metamorphic devolatilization, but some eclogite suites show evidence for fluid-mediated addition of a sedimentary N component (Halama et al., 2010).

The primary goals of this study are (1) to document the concentrations and isotopic compositions of N in hydrated mantle rocks through analyses of samples reflecting different stages of the subduction zone cycle, from oceanic alteration to high-pressure metamorphism,

(2) to assess redistribution and isotope fractionation of N by ultramafic dehydration, and (3) to gain information regarding the source of the fluids responsible for the serpentinization of these mantle rocks. The results place constraints on the extent to which N can be retained in mantle rocks to depths approaching those beneath arcs, information that can be used to calculate a global N subduction flux in ultramafic rocks that can be compared with N fluxes in subducting sediments and basaltic crust.

2. SAMPLING STRATEGY AND SAMPLE LOCATIONS

Serpentinized and metamorphosed mantle peridotites and associated high-pressure veins were investigated from three sites of ultramafic rocks in ophiolite units (Monte Nero/Northern Apennine, Erro Tobbio/Western Alps, Cerro del Almirez/Betic Cordillera), chosen because they record increasing P-T conditions representing the evolution of the hydrated slab mantle from alteration on the ocean floor to subduction metamorphism beyond the breakdown of antigorite serpentine (Fig. 1). Because antigorite contains 12.3 wt.% of H_2O (Schmidt and Poli, 1998), this latter process has been proposed to be responsible for major fluid release in subduction zones (Ulmer and Trommsdorff, 1995; Scambelluri et al., 2001). Although the samples are derived from distinct orogenic terranes, they share petrologic and compositional characteristic as serpentinized mantle rocks and are therefore suitable for investigating progressive dehydration of mantle rocks during subduction. The majority of the samples was petrographically described and analyzed for halogen concentrations by John et al. (2011), and fluid inclusion and oxygen isotope analyses of the samples from Cerro del Almirez were presented in Scambelluri et al. (2004).

2.1. Monte Nero, Northern Apennine, Italy

Serpentinized peridotites from Monte Nero (External Liguride Units) form a several kilometer-sized body and represent pre-subduction oceanic alteration in mantle peridotite (Fig. 1). The Liguride units belong to the Alpine orogenic system and are interpreted as remnants of oceanic and transitional lithosphere of the Western Tethys basin located between the continental margins of Europe and Adria (Marroni et al. 1998; Marroni and Pandolfi, 2007). In the External Ligurides, ultramafic and volcanic rocks occur as large olistoliths within Late Cretaceous sedimentary mélanges (Abbate et al., 1980; Beccaluva et al., 1984). The ultramafic rocks are slices of subcontinental lithospheric mantle emplaced at the surface by early rifting of the ocean basin during the Jurassic (Rampone et al., 1995). They consist of fertile spinel lherzolites with pyroxenite bands (Rampone et al., 1995) and were affected by variable degrees of serpentinization (Rampone et al., 1995). At Monte Nero, olistoliths comprise MORB dikes and gabbroic bodies (Marroni et al., 1998) and Sr and Nd isotope compositions of clinopyroxenes are typical of MORB-type mantle (Rampone et al., 1995). Partial metamorphic re-equilibration in the plagioclase stability field occurred at 164±20 Ma (Rampone et al., 1995). The ultramafic mantle rocks from Monte Nero show several lines of evidence for emplacement into the shallow oceanic lithosphere and fluid influx by serpentinizing fluids: First, they are cut by basaltic dikes, which post-date plagioclase crystallization; second, they are serpentinized and third, they are locally disrupted by breccias consisting of serpentine matrix with serpentinized peridotite clasts (Marroni et al., 1998; Montanini et al., 2006). The degree of serpentinization in the peridotites is variable and reaches up to ~80%. The texturally earliest mineral assemblage consists of porphyroclasts of olivine + orthopyroxene + clinopyroxene with tiny trails of brown spinel. This spinel-facies paragenesis is replaced by a plagioclase-bearing assemblage, resulting in the formation of plagioclase and olivine as reaction products around spinel and replacement of primary porphyroclasts by aggregates of olivine, plagioclase and pyroxenes. Serpentine minerals replace olivine forming mesh-type structures and orthopyroxene forming bastite structures.

XRD analyses reveal that the serpentine minerals are chrysotile and lizardite. The low-grade serpentinites from Monte Nero may represent oceanic serpentinization associated with halogen input from sedimentary sources (John et al., 2011).

2.2. Erro Tobbio, Western Alps, Italy

The Erro Tobbio peridotites are the mantle section of the Voltri massif, which is the largest ophiolite exposure in the European Alps. The pre-subduction history is similar to the Monte Nero peridotites and involves a primary origin as subcontinental mantle, which was exhumed and hydrated during opening of the Jurassic Tethyan ocean basin. Prior to the Jurassic, the pristine peridotites equilibrated at spinel-facies conditions in the subcontinental lithosphere of the Europe-Adria system (Piccardo and Vissers, 2007). Decompressional recrystallization caused the formation of plagioclase- and hornblende-bearing assemblages (Hoogerduijn Strating et al., 1993). During exhumation and emplacement at the seafloor, the peridotites interacted with MORB-type melts (Piccardo and Vissers, 2007). Serpentinization of peridotites and concurrent rodingitization of mafic dikes point to interaction with seawater-derived fluids (Scambelluri et al., 1997). The low-grade serpentinite assemblage consists of chrysotile and/or lizardite, chlorite, magnetite and brucite and indicates serpentinization at temperatures below 300°C (Scambelluri et al., 1997). These low-grade serpentinites are preserved in peridotite volumes that were unaffected by the subduction-related deformation and it is currently debated whether they have been serpentinized on the ocean floor or in the fore-arc mantle wedge (e.g., John et al., 2011, Scambelluri and Tonarini, 2011). During alpine subduction and high-pressure recrystallization, partial dehydration occurred via the reaction:

antigorite + brucite = olivine + fluid (Fig. 1),

which consumes brucite and leaves antigorite in equilibrium with olivine, diopside, chlorite, titanian clinohumite and magnetite as the peak metamorphic assemblage (Scambelluri et al., 2001). Metamorphic veins within the serpentinized peridotites also contain metamorphic olivine and titanian clinohumite. The veins are interpreted to have channelized fluids released at peak metamorphic conditions (Scambelluri et al., 1997) and their composition appears to be controlled by the host rocks (Scambelluri et al., 2001). Based on an eclogitic paragenesis in metagabbros, maximum P-T conditions were estimated at 2-2.5 GPa and 550-600 °C (Messiga et al., 1995). Final exhumation of the Erro Tobbio peridotites occurred during the late stages of Alpine collision.

2.3. Cerro del Almirez, Betic Cordillera, Spain

The chlorite harzburgites from Cerro del Almirez are ultramafic rocks that have been subjected to antigorite dehydration during subduction metamorphism (Fig. 1), representing one of the few field examples of high-pressure breakdown of antigorite (Trommsdorff et al., 1998; Garrido et al., 2005; Padrón-Navarta et al., 2011). The three ultramafic bodies of Cerro del Almirez are part of a ~400m thick and ~2km wide thrust sheet, which comprises antigorite serpentinites and chlorite harzburgites. These ultramafic rocks are interlayered with metapelites and marbles and together they are part of the Nevado-Filábride Complex of the Betic Cordillera (Trommsdorff et al., 1998). The serpentinites are very similar to occurrences of serpentinized peridotites in the Penninic Zone of the Alps. Prograde Alpine subduction zone metamorphism has overprinted previous stages of oceanic hydration and alteration (Trommsdorff et al., 1998; Puga et al., 1999). Within the serpentinites, veins of titanian clinohumite and olivine and minor boudins of rodingite occur. The veins formed at 475°C and 1.3 GPa due to simultaneous breakdown of clinopyroxene and brucite (López Sánchez-Vizcaíno et al., 2009).

The predominant type of chlorite harzburgite has a spinifex-like texture consisting of olivine blades and needles and elongated enstatite in a matrix of chlorite, tremolite and magnetite (Trommsdorff et al., 1998; Puga et al., 1999). Olivine from the spinifex-like textured rocks contain abundant multiphase inclusions containing aqueous fluid and mineral phases that derive from trapping of a homogeneous fluid and precipitated minerals at P-T conditions beyond the stability of antigorite (Scambelluri et al., 2001). Subordinately, a medium- to coarse-grained chlorite harzburgite with granofelsic texture occurs, alternating in meter- to decimeter-scale bodies with the spinifex-like textured rocks throughout the chlorite harzburgite sequence (Padrón-Navarta et al., 2011). Synmetamorphic orthopyroxenite veins with very coarse-grained enstatite, containing the same mineral assemblage as the chlorite harzburgite with very coarse-grained enstatite, occur close to the boundary between serpentinites and harzburgites (López Sánchez-Vizcaíno et al., 2005). The origin of these veins, which have diffuse contacts with the host chlorite harzburgite, is not entirely clear (J.A. Padrón-Navarta, personal communication). The samples analyzed in this study comprise 4 spinifex-textured chlorite harzburgites and 3 orthopyroxene-rich veins.

Thermodynamic calculations show that the serpentinites dehydrated directly to chlorite harzburgite due to a temperature increase from 635 to 695°C at pressures of 1.7-2.0 GPa (López Sánchez-Vizcaíno et al., 2005). Hence, the contact between serpentinites and chlorite harzburgites represents the antigorite-out isograd, which represents the major dehydration reaction:

antigorite = enstatite + olivine + chlorite + fluid (Fig. 1).

This deserpentinization reaction can release significant amounts of water during subduction. At Cerro del Almirez, the H_2O release is limited to about 6-7 wt.% because of the stability of chlorite beyond the antigorite breakdown (Trommsdorff et al., 1998). Peak metamorphic conditions reached by the chlorite harzburgites are ~700 °C and 1.6-1.9 GPa (Puga et al., 1999; Padrón-Navarta et al., 2010). They record the highest metamorphic grade of the sample suite of this study.

3. Analytical methods

3.1. Whole-rock geochemistry

Fused glass discs, prepared from fine-grained whole-rock powders of the ultramafic rocks, were analyzed for major elements and five trace elements (V, Cr, Ni, Zn, Sr) by X-ray fluorescence analysis using a PHILIPS PW 1480 spectrometer at the Institut für Geowissenschaften, Universität Kiel, Germany. The relative standard deviation is typically <0.3% for SiO_2, TiO_2, Al_2O_3, $Fe_2O_3^T$, MnO and CaO, between 0.8 and 1.3% for MgO, Na_2O, K_2O and P_2O_5 and <10% for the trace elements. Averages and uncertainties of reference material analyzed during the course of this study are given in the supplementary material, and long-term reproducibility based on repeat analyses of the BHVO-1 standard were presented by van der Straaten et al. (2008).

3. 2. Nitrogen concentrations and isotopic compositions

Nitrogen contents and isotopic compositions were analyzed at Lehigh University employing the methods described by Bebout et al. (2007) and Li et al. (2007) involving transfer of extracted N (as N_2) into a Finnigan MAT 252 mass spectrometer using a Finnigan Gas Bench II and a U-trap interface in which small samples of N_2 are entrained in a He stream. About 250 mg of sample powder (grain size as fine as ~ 1 μm) were used and tests with analyses of fine-grained powders, involving varying evacuation times and heating regimens for the quartz tubes before sealing, indicate that atmospheric contamination is minimal. Baseline N yields for analyses of 250 mg of fine-grained powder of extremely low-N samples are at blank levels, demonstrating that there is no atmospheric N incorporated beyond blank levels. Based on this testing, all quartz tubes containing samples and Cu/CuO_x reagent are evacuated for ~24 hours before sealing, with intermittent heating to ~100 °C.

Nitrogen extraction is accomplished at 1000 °C, temperatures at which complete N extraction has been demonstrated for metasedimentary rocks, basalts and ultramafic rocks (Bebout et al., 2007; Busigny et al. 2005; Halama et al., 2010; Li et al., 2007; Philippot et al., 2007). All N isotope compositions presented and/or discussed in this paper are reported relative to the composition of atmospheric N_2 (air).

Yields for the gas extractions from unknowns, and thus N concentrations, are obtained by measurement of the *m/z* 28 peak area and using calibrations from analyses of laboratory standards. Uncertainties for N concentrations are usually <5% (Bebout et al., 2007). Measured yields and isotope compositions are corrected for the total system blank, which is largely due to the addition of Cu/CuO_x reagents and reproducible in both size and isotopic composition. During the course of this study, measurements of the reagent blank gave $\delta^{15}N$ = -7.3±1.3‰ (n=10, 1σ) at 153±30 mV on the peak. For peridotite samples, the voltage was typically between 1000 and 3000 mV. Uncertainties in $\delta^{15}N$ are ± 0.15‰ for samples with > 5 µg/g N and ~0.6‰ for samples with 1-2 µg/g N. One sample with <1 µg/g N required such a substantial blank correction that the resulting $\delta^{15}N$ value is considered less reliable and thus is not reported. The accuracy of the $\delta^{15}N$ measurements was evaluated by repeat measurements of two reference materials, a fuchsite (Cr-rich phengitic white mica; # 2-1-36) and a blueschist (# 9150) (Bebout et al., 2007). The results ($\delta^{15}N$ = +2.4±0.2‰ (n=10, 1σ) for # 2-1-36 and 2.5±0.3‰ (n=13, 1σ) for # 9150 agree well with previous measurements (Bebout, 1997; Bebout et al, 2007).

Previous experiments on ultramafic rocks used a slightly different technique, where samples were pre-heated and degassed at 450 °C, in the presence of oxygen, in order to remove organic contamination and atmospheric N (Philippot et al., 2007; Busigny et al., 2005). It is conceivable that, in the case of hydrated ultramafic rocks, this procedure also removes some N from the rock matrix and thereby fractionates N isotopes. The different analytical protocols could explain some of the difference between our results and the work by Philippot et al. (2007; see Fig. 2); however, experimental testing for partial N loss at low temperatures would clearly be necessary to further evaluate this possibility. Alternatively, and also quite conceivably, sample heterogeneity could be responsible for the variations in $\delta^{15}N$.

4. Results

Nitrogen concentrations and $\delta^{15}N$ are presented in Table 1 and Fig.2, and the major and trace element contents of the bulk samples are listed in the supplementary material. Figure 3 shows the relationship between the N elemental and isotopic signatures with loss on ignition (LOI) and frequency distribution diagrams (Figs. 4 and 5) summarize the $\delta^{15}N$ of the samples and other subduction-related rocks. Overall, all ultramafic rocks investigated have N concentrations that are elevated compared to the depleted MORB source mantle (0.27±0.16 µg/g; Marty and Dauphas, 2003) and they are quite variable in $\delta^{15}N$, with an overall range of -4 to +5‰ (Table 1, Fig. 2). For the massive serpentinites reflecting different degrees of hydration and rehydration, there is no systematic variation of N content or $\delta^{15}N$ with rock type, major element chemistry or LOI (Figs. 2 and 3).

4. 1. Low-grade serpentinites

Low-grade serpentinites from Monte Nero (samples MNS 1-4) have moderately high contents of Al_2O_3 (1.9-3.4 wt.%) and CaO (0.95-2.95 wt.%; see supplementary material). The variable values for LOI (5.7-9.9 wt.%) reflect different degrees of serpentinization. The four samples cover a wide range in $\delta^{15}N$ (-3.8 to +2.8‰; Fig. 2), with the lowest values overlapping the depleted mantle composition (-5±2; Marty and Dauphas, 2003) and the heavier values within the range of modern marine sediments ($\delta^{15}N$ = -2 to +10; Fig. 5).

Nitrogen concentrations of the low-grade serpentinites from Monte Nero are low (1.3-2.1 μg/g).

The low-grade serpentinites from Erro Tobbio (samples ET Cl-2 and ET Cl-3) are similar in major element composition to those from Monte Nero, but are characterized by slightly more positive $\delta^{15}N$ values (+3.1 to +3.5‰) and higher N concentrations (2.7-4.5 μg/g). Their N isotopic compositions fall into the range for modern marine sediments and subduction-related metasediments ($\delta^{15}N$ = 0 to +12‰; Fig. 5).

4. 2. High-pressure serpentinites

The high-pressure serpentinites from Erro Tobbio have moderate Al_2O_3 (1.5-2.9 wt.%) and CaO (0.84-1.78 wt.%) contents and high LOI values (7.6-11.9 wt.%; see supplementary material). The positive $\delta^{15}N$ values (+1.6 to +4.7‰) with a weighted average of +3.4‰ overlap with the low-grade serpentinites (Table 1, Fig. 4) and there appears to be a positive correlation between [N] and $\delta^{15}N$ (Fig. 2). The high-pressure veins within the Erro Tobbio serpentinites have MgO contents broadly similar to their host rocks, but $Fe_2O_3^T$ contents are higher and Al_2O_3 ($\leq$ 1wt.%) and LOI are significantly lower. Three pairs of host HP serpentinites and associated veins show a systematic difference in $\delta^{15}N$, with the veins isotopically lighter by 2.2±0.6‰ (Table 1; Fig. 3). Nitrogen concentrations, however, do not show a systematic difference between serpentinites and veins.

4. 3. Chlorite harzburgites

The chlorite harzburgites from Cerro del Almirez have Al_2O_3 contents (2.0-3.2 wt.%) that are similar to the low-grade and high-pressure serpentinites, but their CaO contents (0.05-0.07 wt.%) and LOI values (4.0-4.9 wt.%) are significantly lower, whereas SiO_2 is slightly enriched (up to 45 wt.%). Nitrogen concentrations scatter between 1.7 and 4.3 μg/g for three samples, but one chlorite harzburgite is exceptionally enriched in N with 21 μg/g (Table 1, Fig. 2). The weighted average in $\delta^{15}N$ is +1.1‰, but the range is considerable (-2.4 to +2.7‰) and completely overlaps with low-grade serpentinites. The Cerro del Almirez veins have relatively high Al_2O_3 (3.1-4.3 wt.%) and low CaO (0.06-0.13 wt.%) contents. Nitrogen concentrations (1.3-4.0 μg/g) and $\delta^{15}N$ of the veins largely overlap with the chlorite harzburgites, but the veins are, on average, isotopically heavier (weighted average for $\delta^{15}N$ = +3.1‰).

5. Discussion

5. 1. Nitrogen in ultramafic rocks

Based on studies of various igneous mantle-derived rocks and diamonds, the Earth's mantle appears to be heterogeneous in its N isotopic composition and its N concentration. Negative $\delta^{15}N$ values in diamonds and MORBs demonstrate that the mantle contains non-atmospheric N (Cartigny et al., 1998; Marty and Zimmermann, 1999). However, it is disputed whether subduction processes are the key factor for producing some of the variability (Dauphas and Marty, 1999; Jia et al., 2003) or whether degassing and fractionation within the mantle are the main cause for these variations (Cartigny et al., 2001b). Estimates for the N concentration in the mantle range from 0.27 to 40 μg/g (Cartigny et al., 2001a; Marty and Dauphas, 2003), with peridotite xenolith data scattering at the lower end of this range (0.1-0.8 μg/g N; Yokochi et al., 2009). The $\delta^{15}N$ of the depleted mantle is around -5‰ (Marty and Dauphas, 2003; Cartigny et al., 2001), whereas enriched plume mantle is thought to be characterized by a positive $\delta^{15}N$ value of about +3‰ reflecting incorporation of heavy N from recycled subducted slabs (Marty and Dauphas, 2003).

Orogenic peridotites represent an important source of information regarding the chemistry of the Earth's mantle. Previously analyzed serpentinized peridotites contain 1-15 μg/g N (Philippot et al., 2007; Halama et al., 2010), consistent with the data obtained in this study. However, it is not clear whether the large variability in N contents observed is inherited from the primary mantle rocks, or whether is due to the effects of seafloor alteration or subduction-zone metamorphism. The lack of any significant correlation of N contents with metamorphic grade and the large overlap in $\delta^{15}N$ values between low-grade serpentinites, HP serpentinites and chlorite harzburgites suggest that the variability in N concentrations is a feature from a pre-subduction or early subduction stage. Here, we consider whether this variability is inherited from a heterogeneous mantle or is due to addition of sedimentary-organic N during serpentinization. Addition of N to hydrating slab ultramafic rocks could conceivably occur in the outer rise region or in shallow parts of the forearc, along normal faults produced during slab bending. Alternatively, N could be added to mantle wedge ultramafic rocks by H_2O-rich fluids liberated during forearc devolatilization reactions.

Some of the low-grade serpentinites (samples MNS-2 and MNS-3 from Monte Nero) overlap in $\delta^{15}N$ with what are considered typical depleted mantle N isotopic compositions. Hence, they are interpreted to preserve a primary mantle signature with no significant effects of serpentinization and metamorphism. The positive $\delta^{15}N$ values of the other low-grade serpentinites (samples MNS-1 and MNS-4 from Monte Nero and samples ET Cl-2 and ET Cl-3 from Erro Tobbio) likely reflect N input and related N isotopic changes due to interaction with serpentinizing fluids. For those samples, a plume mantle origin can be discarded because of LREE-depleted REE patterns typical for depleted mantle (Scambelluri et al., 2001) and, in case of Monte Nero, depleted Sr-Nd isotopic compositions (Rampone et al., 1995) and the close spatial association to peridotite samples with negative $\delta^{15}N$ values representing depleted mantle.

The weighted average of the HP peridotites ($\delta^{15}N$ = +3.3‰) and the positive $\delta^{15}N$ values of the chlorite harzburgites (weighted average of $\delta^{15}N$ = +1.1‰) overlap with subduction-related metasediments and are also very similar to mafic eclogites and blueschists (Fig. 4). The positive $\delta^{15}N$ values of HP peridotites from Erro Tobbio are unlikely to reflect primary mantle, since the REE patterns indicate a depleted mantle source (Scambelluri et al., 2001) for which negative $\delta^{15}N$ values are expected. In agreement with observations based on noble gas data (Kendrick et al., 2011) and halogen concentrations (John et al., 2011), they are interpreted to reflect addition of N from organic-sedimentary sources via serpentinizing fluids before or during the early stages of subduction. Moreover, the weak positive correlation between [N] and $\delta^{15}N$ in the Erro Tobbio samples indicates that addition of N is coupled to an increase in $\delta^{15}N$. The interpretation of N input by serpentinizing fluids also applies to the positive $\delta^{15}N$ values of HP peridotites from Ecuador, which represent oceanic lithospheric mantle with a relative LREE depletion, although some metasomatized eclogites from this locality have also been affected by a high-pressure fluid-mediated overprint (John et al., 2010; Halama et al., 2010; 2011).

In contrast to the LREE-depleted serpentinites, chondrite-normalized REE patterns of the Cerro del Almirez chlorite harzburgites are moderately U-shaped with only a slight depletion of LREE relative to HREE (Garrido et al., 2005). These harzburgites and associated serpentinites with relatively flat REE patterns (Garrido et al., 2005) represent mantle of sub-continental lithospheric origin (Trommsdorff et al. 1998, Gómez-Pugnaire et al. 2000), but it is difficult to distinguish between a primary positive $\delta^{15}N$ signal, potentially from a plume mantle source, or derivation of the positive $\delta^{15}N$ value due to pre-subduction hydration. The grossly different N concentrations in the Cerro del Almirez samples, however, are more consistent with different degrees of N addition. Assuming that the peridotite xenoliths analyzed for N (Yokochi et al., 2009) represent the pristine mantle with some heterogeneity in

N concentrations (0.1-0.8 μg/g N), the large variability in N contents in the chlorite harzburgites (1.7–20.6 μg/g N) is more consistent with variable interaction with serpentinizing fluids than inheritance from a heterogeneous mantle source. A comparable conclusion was reached for high-pressure metamorphosed basaltic rocks, which largely reflect the N contents and $\delta^{15}N$ values of AOC (Halama et al., 2010). Importantly, the majority of the ultramafic mantle rocks that have experienced HP subduction have positive $\delta^{15}N$ values, so that the preferred interpretation for this observation is adding N during serpentinization and hydration on the seafloor or during the early stages of subduction. The available data are consistent with addition of N with organic-sedimentary origin during exposure of the ultramafic rocks on the seafloor, during slab bending and related circulation of fluids through the oceanic mantle (Ranero et al., 2003; Halama et al., 2010; John et al., 2011) or in the fore-arc mantle wedge. Based on the available evidence, it appears unlikely that the positive $\delta^{15}N$ values represent a primary mantle feature.

5. 2. Behavior of nitrogen during dehydration

Comparisons between low-grade and high-grade rocks and between host rocks and veins can provide information regarding the behavior of N and potential isotopic fractionation during dehydration. Increasing $\delta^{15}N$ with increasing metamorphic grade in some metasedimentary suites was interpreted to reflect dehydration of N-bearing silicates at the higher grades (e.g., Bebout and Fogel, 1992; Mingram and Bräuer, 2001). However, other metasedimentary suites with large ranges in metamorphic grade show relatively little shift in N concentration and $\delta^{15}N$ with increasing grade. Busigny et al. (2003) suggested that the apparent lack of N loss, and related isotopic shift, in a Western Alps metasedimentary traverse reflects subduction of the rocks along very low temperature prograde P-T paths, resulting in little devolatilization. Pitcairn et al. (2005) noted little systematic change in N concentration and $\delta^{15}N$ with increasing grade in the Otago and Alpine Schists, New Zealand, and suggested that some subtle N isotope variation in these rocks could reflect maturation of kerogen (i.e. the transformation of kerogen-bound C-H-N compounds to NH_4^+ structurally sited in K-bearing minerals) or multiple metamorphic episodes rather then dehydration of silicates. Systematic trends in [N] and $\delta^{15}N$ are absent not only in metabasalts and metagabbros investigated by Halama et al. (2010) and Busigny et al. (2011), but also in the ultramafic rocks of this study. The lack of evidence for loss of N in these ultramafic rocks warrants further discussion.

For metasedimentary rocks, it is well established that N is largely fixed as NH_4^+ in micas and hence the stability of mica strongly influences the release of N during subduction. Determining the mineral residency of N in ultramafic rocks is more difficult because of the lack of potassic phases, which commonly serve as hosts for N (because of the similarity of K^+ and NH_4^+ in charge and ionic radius), and because N occurs in these rocks at only trace concentrations. It appears unlikely that N is hosted in the mineral lattice of serpentine minerals or chlorite, based on the crystal chemistry of these phases. However, tremolite could in some cases contain some N, and the tremolite in some Almirez samples contains up to 0.53 wt. % K_2O (J. A. Padrón-Navarta, personal communication). Another possibility is that N could reside in sealed voids and cracks produced during serpentinization (Philippot et al., 2007), as has been proposed for NaCl derived from seawater (Sharp and Barnes, 2004). A possibility that was advocated for noble gas retention in HP ultramafic rocks is the leakage of H^+ out of fluid inclusions by diffusion and the retention of heavier solutes in the desiccated inclusions (Kendrick et al., 2011). If that is the case for N in chlorite harzburgites, the N budget would represent a mixture of rock residue and incorporated fluid. A variable N contribution by fluid inclusions is consistent with the common occurrence of inclusions in the chlorite harzburgites (Scambelluri et al., 2001) and the highly variable N contents (Table 1).

Three pairs of host HP serpentinites and associated veins from Erro Tobbio show a systematic difference in $\delta^{15}N$, with the veins isotopically lighter by 2.2±0.6‰ (Fig. 3), in agreement with residual N in the host rock becoming heavier due to preferential release of ^{14}N by dehydration reactions (Haendel et al., 1986; Bebout and Fogel, 1992). Based on the fractionation factors for N_2-NH_4^+ exchange given by Hanschmann (1981) the calculated $\Delta^{15}N_{fluid\text{-}rock}$ ($\Delta^{15}N = \delta^{15}N_{fluid}-\delta^{15}N_{rock}$) would be ~ -2.2‰ for peak temperature conditions at Erro Tobbio. This concordance between calculated and measured N isotope fractionation supports an origin of these veins by dehydration, assuming that the veins reflect the fluid N isotope composition. In contrast, the orthopyroxene-rich veins from Cerro del Almirez are slightly heavier than the associated chlorite harzburgites. This lack of a systematic change in $\delta^{15}N$ between host peridotites and veins (Fig. 4) with degree of water uptake and release does not indicate significant (>5‰) N isotope fractionation during dehydration. However, nitrogen isotopic changes due to dehydration may have been overprinted by the influx of N from metasediments during exhumation, as the ultramafic suites are associated with or enclosed within metasedimentary rocks. Such an influx of an exhumation-related, metasediment-derived fluid appears highly unlikely because field, petrographic and independent geochemical evidence for interaction with the respective metasedimentary units is lacking. Alternatively, the non-systematic relationship of the orthopyroxenite veins and their host rocks at Cerro del Almirez could be unrelated to dehydration processes, in which case no dehydration-related N isotope fractionation would be expected. To conclude, if the observed N isotope fractionation between veins and host rocks at Erro Tobbio is due to dehydration reactions, its effect is still small (< 3‰) relative to the variability in $\delta^{15}N$ observed on outcrop scale.

5. 3. The isotopic composition of nitrogen in the subducted slab

The determination of $\delta^{15}N$ values in ultramafic rocks with both a pre-subduction signature and a HP subduction signature (Fig. 4) allows an assessment of the role of N stored in ultramafic rocks and how the ultramafic rocks affect the total N budget in the subducting slab. Although there is a significant variability in N concentrations, $\delta^{15}N$ and thickness of the lithologies depending on the subduction zone investigated, a global approach is justified because there is currently no present-day subduction zone where all lithologies have been investigated for [N] and $\delta^{15}N$, and subduction-related metamorphosed rocks where N data are available for all lithologies (Halama et al., 2010) only provide information regarding paleo-subduction. A compilation of [N] and $\delta^{15}N$ data for marine sediments, metasediments, oceanic lithosphere and metamorphosed oceanic lithosphere (Table 2) reveals that nearly all lithologies have positive $\delta^{15}N$ values. Regarding the average values listed, key features of a comparison between unmetamorphosed and metamorphosed rocks are discussed in the following paragraphs.

For the sediments/metasediments, metamorphosed rocks tend to have lower [N] and lower $\delta^{15}N$ values (Table 2, Fig. 5). Two explanations for this observation have been put forward (Sadofsky and Bebout, 2003; 2004). First, most of the metasedimentary rocks investigated are derived from trench sediments and accretionary prisms that are characterized by enhanced contributions of terrestrial organic matter with a relatively low $\delta^{15}N$ (+1.8; Minoura et al., 1997) compared to the marine component with $\delta^{15}N$ ~ +8. Hence, the difference in $\delta^{15}N$ between unmetamorphosed and metamorphosed sediments is likely attributable to greater proportions of terrestrial organic matter in the sedimentary protoliths (Sadofsky and Bebout, 2004). A second explanation is the loss of a high-$\delta^{15}N$ component, perhaps as nitrate (NO^{3-}), during diagenesis. This possibility is supported by experimental studies, which suggest that a negative shift in $\delta^{15}N$ by about 1-3‰ may be common in oceanic sediments (Lehmann et al., 2002).

Nitrogen concentrations of the oceanic lithosphere upper mantle section are one to two orders of magnitude lower than those of (meta)sediments, and they are broadly similar for the unmetamorphosed rocks and their metamorphosed equivalents. Nitrogen isotopic compositions are quite variable, but negative δ^{15}N values are conspicuously lacking for samples of metamorphosed oceanic lithosphere (Table 2, Fig. 5). Because the depleted mantle and igneous rocks derived from the depleted mantle are associated with a negative δ^{15}N signature of ~5‰ (Cartigny et al., 1998; Marty and Dauphas, 2003), this feature, observed for a variety of samples from different localities, suggests uptake of N from a sedimentary-organic source. Incorporation of sedimentary-organic N in serpentinized ultramafic rocks is expected to occur in oceanic slab mantle, at transform or bending-related faults, and in the forearc mantle wedge, for the latter setting resulting from infiltration by H_2O-rich fluids emanating from subducting slabs. There are very few N data available for subduction-related ultramafic rocks (Philippot et al., 2007; this study), and the exact setting (slab mantle or mantle wedge) is somewhat uncertain for at least the Erro Tobbio rocks. Given the uncertainties, we suggest that it is valid, as a first pass, to consider our data as representing plausible compositions of subducting slab mantle that could, at greater depths, dehydrate and release its N into the subarc mantle wedge or retain this N to greater depths in the mantle. Additions of sedimentary-organic N to ultramafic rocks in either setting would in general tend to produce δ^{15}N values higher than those of the upper, depleted mantle (near -5‰) and likely >0‰.

Estimates of the global contributions of the three major lithologies in a subducting slab – marine sediment, igneous oceanic crust and serpentinized mantle – show that the amount of N stored in serpentinized ultramafic rocks is relatively small (Fig. 6). An average thickness of 500 m serpentinized mantle would carry into the subduction zone about two orders of magnitude less N than a sediment section of similar thickness. For the igneous oceanic crust, the degree of alteration is important as AOC tends to be enriched in N compared to fresh

MORB (Busigny et al., 2005; Li et al., 2007). Thus, a completely altered section of crust may transport an amount of N comparable to that of the sedimentary rocks into the subduction zone (Table 3).

For a typical section of the incoming plate with 500 m of sediment, 6 km of igneous crust and 500 m of serpentinized mantle, contributions of 86%, 13% and 1% were calculated (Fig. 6), resulting in an average $\delta^{15}N$ value of +4.9‰. The 86% fraction delivered by sediments is similar to the sedimentary N contribution to the Central American Arc (~80% of subducted N; Li and Bebout, 2005), whereas a considerably smaller sedimentary contribution of ~33% of the total subducted N was estimated for the Izu-Bonin-Mariana arc system (Mitchell et al., 2010). The great variability from margin to margin in terms of diverse thicknesses of the lithological units and significant variability in N contents for different sediment types allows for large differences in these estimates, and a more complete data base is clearly desirable. One critical factor in comparing the values for different trenches with global values is the amount of sediment scraped off during the early stages of subduction and incorporated into an accretionary prism. If, in the model slab section, the thickness of subducted sediment is reduced by a factor of 5 (case B in Table 3), its contribution would be reduced to 55% and the total slab $\delta^{15}N$ would be +2.8‰. If, on the other hand, a greater depth of serpentinization (10 km; case C in Table 3) is taken into account (Ranero et al., 2003), the contribution of ultramafic mantle rocks to the overall N budget increases to 12% and results in a bulk slab $\delta^{15}N$ values of +4.5‰ (Fig. 6). For the ultramafic mantle rocks, the key point is that the amount of serpentinization is an important parameter regarding the overall contribution of these rocks to the subduction volatiles budgets. As argued earlier in the text, the N elemental and isotopic signature of serpentinized ultramafic rocks in slab mantle and forearc mantle is likely to be similar, but the amount of serpentinization is largely unknown, in particular for the hydrated wedge mantle. By assuming differing amounts of serpentinized slab mantle rock in the calculations and evaluating the effect on the N flux, scenarios with or without down-dragged forearc wedge mantle are accounted for. Despite significant uncertainties associated with the calculations, the overall picture emerging, based on presently available data, is that the globally subducted N has a positive $\delta^{15}N$ value of approximately +4±1‰.

By combining the thicknesses of the different lithological units of the incoming slab with N data from metamorphosed rocks, a metamorphosed equivalent of a typical subducting plate section is obtained. The calculated bulk $\delta^{15}N$ of the metamorphosed slab is +3.2‰, a decrease of 1.7‰ compared to the unmetamorphosed slab entering the subduction zone, largely reflecting the effect of decreasing $\delta^{15}N$ values in metasediments compared with their unmetamorphosed protoliths. The metamorphosed crust and mantle parts have a more significant influence on this value than in the unmetamorphosed case, but it is still the $\delta^{15}N$ of the metasediments that exerts the most prominent influence. However, a reduced sediment thickness of 100 m in the metamorphosed slab would result in a bulk slab $\delta^{15}N$ value of +3.9‰, dominated by the contribution of metamorphosed oceanic crust (55%). Assuming that the metamorphosed slab is representative for the residual N after dehydration, the calculations for the N budget ($\delta^{15}N$ = 3.2-3.9‰) can be compared to results for the Izu-Bonin-Mariana arc, where the residual N subducted into the mantle was estimated at $\delta^{15}N$ = -1.9‰, based on estimates of the relative contribution of sediment and AOC to the arc volcanic output (Mitchell et al., 2010). This difference is the result of a relatively small sedimentary N contribution to the total subducted N budget at the Izu-Bonin-Mariana arc and relatively light N isotopic compositions of the AOC in front of the Izu-Bonin-Mariana trench compared to other sites (see Table 2).

5. 4. Implications for global nitrogen recycling

The N isotope composition of the residual slab is important for two aspects of global N cycling. First, it is crucial to the interpretation that positive $\delta^{15}N$ values in plume-related igneous rocks were derived from mantle sources that contain recycled material (Tolstikhin and Marty, 1998; Marty and Dauphas, 2003; Fischer et al., 2005). Second, models that attempt to explain the N isotopic imbalance between the Earth's external and internal reservoirs require that N delivered into the mantle is enriched in ^{15}N (Cartigny et al., 1998; Javoy, 1997, 1998; Tolstikhin and Marty, 1998).

Igneous rocks that are sourced from the deep mantle are characterized by positive $\delta^{15}N$ values. For instance, ultrapotassic rocks from India show a range in $\delta^{15}N$ from +1.6 to +8.7 (Jia et al., 2003), and ultramafic rocks and carbonatites from the Kola Peninsula have $\delta^{15}N$ of -0.2 to +6.5 (Dauphas and Marty, 2003). Both suites show no evidence of crustal contamination, so that their N isotopic composition was interpreted to reflect the recycling of crustal material into the deep mantle and incorporation of this isotopic signature in the mantle melts. The positive $\delta^{15}N$ values determined for individual lithological components of the metamorphosed slab and for the bulk slab (Table 3) shows that at least up to depths of about 70 km, subducted components preserve a positive $\delta^{15}N$ signature. If this signature is representative of subducted material that enters the deep mantle beyond sub-arc depths, it may well provide a source of heavy N in plume-related rocks.

Since formation of the Earth, N had to be recycled into the mantle in significant amounts to drive the mantle's N isotopic composition from an initial $\delta^{15}N$ value of -30‰ to the present-day $\delta^{15}N$ value of -5‰ (Javoy, 1997; Tolstikhin and Marty, 1998). Models of volatile recycling show that significant trapping on N by the mantle during the Earth's history must have occurred (Javoy, 1997). Accumulation of N in the mantle could have been aided by the presence of osbornite (TiN) as stable mantle nitride (Dobrzhinetskaya et al., 2009) or by the formation of high-pressure K-phases, which are expected to be able to incorporate large amounts of NH_4^+ into their structures, thus providing a means for N transport into the deep mantle (Watenpuhl et al., 2010). The N isotopic evolution of the mantle requires subduction of an isotopically heavy component, in agreement with the calculated $\delta^{15}N$ of the bulk metamorphosed slab. Thus despite significant local variations in the $\delta^{15}N$ values of subducted material (e.g. Mitchell et al., 2010), a globalization of the available data points to a positive $\delta^{15}N$ of material that is subducted into the deep mantle.

The estimates of the total flux of subducted N (Table 3) for a typical slab section are in good agreement for the pre-subduction (3.3 x 10^{10} mol/year) and the metamorphosed (3.9 x 10^{10} mol/year) slab. These values are also close to the 4.5 x 10^{10} mol/year estimate from Hilton et al. (2002). The individual flux estimates for the sediment and the igneous crustal sections of the slab are also similar to those of Busigny et al. (2011). These fluxes of subducted N are larger than the amount of excess (non-atmospheric) N_2 emitted from arc volcanoes, implying that a significant amount of N may not reach the zones of arc magma generation and/or is retained in the deeper mantle (Hilton et al., 2002). The retention of N in subducted oceanic crust (Busigny et al., 2011; Halama et al., 2010) and in serpentinized peridotites (this study) up to depths of about 70 km suggests that at least some N reaches the deep mantle, where it may later be mobilized in mantle plumes.

6. Conclusions

The investigation of serpentinized peridotites, reflecting different stages of subduction zone metamorphism, and the integration of these data with those from sedimentary and mafic igneous rocks, are summarized in the following conclusions:

1. Low-grade serpentinized peridotites that formed during early stages of subduction have variable $\delta^{15}N$ values. At the lower end, $\delta^{15}N$ values are close to the composition of the

depleted mantle (-5‰), whereas the isotopically heavier values overlap with those typical of modern marine sediments as well as metamorphosed sedimentary rocks. This suggests an addition of organic-sedimentary N to the peridotites, incorporated via serpentinization during bending–related faulting of the slab and/or via metasomatic additions during hydration in the forearc mantle wedge.

2. Nitrogen is retained in HP peridotites down to depths of at least 60-70 km, and there is apparently no significant loss of N due to dehydration. The $\delta^{15}N$ of N subducted in serpentinized ultramafic rocks to sub-arc depths, and possibly beyond, is about +1 to +4‰. This N isotopic signature is interpreted to derive from interaction of ultramafic rocks with serpentinizing fluids, which carry a sedimentary N isotope signature, before and/or in the early stages of subduction. This sedimentary signature is largely preserved during prograde dehydration of the slab. Hence, the N system provides a great example of how serpentinite and sediment-derived components can mix during the subduction cycle.

3. A systematic decrease of $\delta^{15}N$ values is observed in veins from the Erro Tobbio peridotite body compared to their host rocks, suggesting equilibrium N isotope fractionation during fluid release. However, this fractionation is small relative to inherited inhomogeneities in the N isotopic composition due to variable degrees of serpentinization by fluids.

4. The contribution of N stored in serpentinized ultramafic rocks to the budget of subducting N is small (1-12%) compared to the amount of N in sediments and altered oceanic crust.

5. Based on the combined data for an unmetamorphosed and a high-pressure metamorphosed typical slab section, the isotopic composition of subducted N can be estimated at +4±1‰. This positive $\delta^{15}N$ value is in agreement with models for the evolution of volatiles on Earth and with the concept of recycling of subducted N in mantle plumes.

Acknowledgments

We thank P. Appel and A. Weinkauf for help with XRF measurements. J. A. Padrón-Navarta and E. Mitchell are thanked for constructive reviews, and the editorial handling of E. Suess and W.-C. Dullo is appreciated. Support of this project was partly provided by National Science Foundation grant EAR-0711355 to GEB and by the Italian MIUR to MS. This is contribution no. 222 of the Sonderforschungsbereich (SFB) 574 "Volatiles and Fluids in Subduction Zones" at Kiel University.

References

Abbate E, Bortolotti V, Principe G (1980) Apennines ophiolites: a peculiar oceanic crust. In: Rocci G (ed) Tethyan ophiolites, western area, Ofioliti Special Issue vol 1. pp 59-96

Bebout GE (1997) Nitrogen isotope tracers of high-temperature fluid-rock interactions: Case study of the Catalina Schist, California. Earth and Planetary Science Letters 151:77-90

Bebout GE (2007) Metamorphic chemical geodynamics of subduction zones. Earth and Planetary Science Letters 260:373-393

Bebout GE, Fogel ML (1992) Nitrogen-isotope compositions of metasedimentary rocks in the Catalina Schist, California: Implications for metamorphic devolatilization history. Geochimica et Cosmochimica Acta 56:2839-2849

Beccaluva L, Macciotta G, Piccardo GB, Zeda O (1984) Petrology of lherzolitic rocks from Northern Apennine ophiolites. Lithos 17:299-316

Busigny V, Cartigny P, Philippot P, Ader M, Javoy M (2003) Massive recycling of nitrogen and other fluid-mobile elements (K, Rb, Cs, H) in a cold slab environment: evidence from HP to UHP oceanic metasediments of the Schistes Lustrés nappe (western Alps, Europe). Earth and Planetary Science Letters 215:27-42

Busigny V, Cartigny P, Philippot P (2011) Nitrogen isotopes in ophiolitic metagabbros: A re-evaluation of modern nitrogen fluxes in subduction zones and implication for the early Earth atmosphere. Geochimica et Cosmochimica Acta 75:7502-7521

Busigny V, Laverne C, Bonifacie M (2005) Nitrogen content and isotopic composition of oceanic crust at a superfast spreading ridge: A profile in altered basalts from ODP Site 1256, Leg 206. Geochemistry Geophysics Geosystems 6: Q12O01, doi:10.1029/2005GC001020

Cartigny P, Harris JW, Javoy M (2001a) Diamond genesis, mantle fractionations and mantle nitrogen content: a study of δ^{13}C-N concentrations in diamonds. Earth and Planetary Science Letters 185:85-98

Cartigny P, Harris JW, Phillips D, Girard M, Javoy M (1998) Subduction-related diamonds? - The evidence for a mantle-derived origin from coupled δ^{13}C-δ^{15}N determinations. Chemical Geology 147:147-159

Cartigny P, Jendrzejewski N, Pineau F, Petit E, Javoy M (2001b) Volatile (C, N, Ar) variability in MORB and the respective roles of mantle and source heterogeneity and degassing: the case of the Southwest Indian Ridge. Earth and Planetary Science Letters 194:241-257

Dauphas N, Marty B (1999) Heavy nitrogen in carbonatites of the Kola Peninsula: A possible signature of the deep mantle. Science 286:2488-2490

Dobrzhinetskaya LF, Wirth R, Yang J, Hutcheon ID, Weber PK, Green HW (2009) High-pressure highly reduced nitrides and oxides from chromitite of a Tibetan ophiolite. Proceedings of the National Academy of Sciences 106:19233-19238

Elkins LJ, Fischer TP, Hilton DR, Sharp ZD, McKnight S, Walker J (2006) Tracing nitrogen in volcanic and geothermal volatiles from the Nicaraguan volcanic front. Geochimica et Cosmochimica Acta 70:5215-5235

Fischer TP, Hilton DR, Zimmer MM, Shaw AM, Sharp ZD, Walker JA (2002) Subduction and recycling of nitrogen along the Central American margin. Science 297:1154-1157

Fischer TP, Takahata N, Sano Y, Sumino H, Hilton DR (2005) Nitrogen isotopes of the mantle: Insights from mineral separates. Geophysical Research Letters 32, doi:10.1029/2005GL022792

Garrido CJ, López Sánchez-Vizcaíno VL, Gómez-Pugnaire MT, Trommsdorff V, Alard O, Bodinier J-L, Godard M (2005) Enrichment of HFSE in chlorite-harzburgite produced by high-pressure dehydration of antigorite-serpentinite: Implications for subduction magmatism. Geochemistry Geophysics Geosystems 6: Q01J15, doi:10.1029/2004GC000791

Gómez-Pugnaire MT, Ulmer P, López Sánchez-Vizcaíno V (2000) Petrogenesis of the mafic igneous rocks of the Betic Cordilleras: A field, petrological and geochemical study. Contributions to Mineralogy and Petrology 139:436-457

Haendel D, Mühle K, Nitzsche H-M, Stiehl G, Wand U (1986) Isotopic variations of the fixed nitrogen in metamorphic rocks. Geochimica et Cosmochimica Acta 50:749-758

Hacker BR, Abers GA, Peacock SM (2003) Subduction factory 1. Theoretical mineralogy, densities, seismic wave speeds, and H_2O contents. Journal of Geophysical Research 108 (B1), 2029, doi:10.1029/2001JB001127

Halama R, Bebout GE, John T, Schenk V (2010) Nitrogen recycling in subducted oceanic lithosphere: The record in high- and ultrahigh-pressure metabasaltic rocks. Geochimica et Cosmochimica Acta 74:1636-1652

Halama R, John T, Herms P, Hauff F, Schenk V (2011) A stable (Li, O) and radiogenic (Sr, Nd) isotope perspective on metasomatic processes in a subducting slab. Chemical Geology 281:151-166

Hanschmann G (1981) Berechnung von Isotopieeffekten auf quantenchemischer Grundlage am Beispiel stickstoffhaltiger Moleküle. ZFI Mitteilungen 41:19-39

Hilton DR, Fischer TP, Marty B (2002) Noble gases and volatile recycling at subduction zones. In: Porcelli D, Ballentine CJ, Wieler R (eds) Noble gases in geochemistry and cosmochemistry, Reviews in Mineralogy and Geochemistry vol 47. The Mineralogical Society of America, Washington, DC, pp 319-370

Javoy M (1997) The major volatile elements of the Earth: Their origin, behavior, and fate. Geophysical Research Letters 24:177-180

Javoy M (1998) The birth of the Earth's atmosphere: the behaviour and fate of its major elements. Chemical Geology 147:11-25

Jia Y, Kerrich R, Gupta AK, Fyfe WS (2003) ^{15}N-enriched Gondwana lamproites, eastern India: Crustal N in the mantle source. Earth and Planetary Science Letters 215:43-56

John T, Scambelluri M, Frische M, Barnes JD, Bach W (2011) Dehydration of subducting serpentinite: Implications for halogen mobility in subduction zones and the deep halogen cycle. Earth and Planetary Science Letters 308:65-76

John T, Scherer E, Schenk V, Herms P, Halama R, Garbe-Schönberg D (2010) Subducted seamounts in an eclogite-facies ophiolite sequence: The Andean Raspas Complex, SW Ecuador. Contributions to Mineralogy and Petrology 159:265-284

Johnson ER, Wallace PJ, Delgado Granados H, Manea VC, Kent AJR, Bindeman IN, Donegan CS (2009) Subduction-related volatile recycling and magma generation beneath Central Mexico: Insights from melt inclusions, oxygen isotopes and geodynamic models. Journal of Petrology 20:1729-1764

Kendrick MA, Scambelluri M, Honda M, Phillips D (2011) High abundances of noble gas and chlorine delivered to the mantle by serpentinite subduction. Nature Geoscience 4:807-812

Kerrich R, Jia Y, Manikyamba C, Naqvi SM (2006) Secular variations of N-isotopes in terrestrial reservoirs and ore deposits. In: Kesler SE, Ohmoto H (eds) Evolution of Early Earth's Atmosphere, Hydrosphere, and Biosphere - Constraints from ore deposits. Geological Society of America, pp 81-104

Lehmann MF, Bernasconi SM, Barbieri A, McKenzie JA (2002) Preservation of organic matter and alteration of its carbon and nitrogen isotope composition during simulated and in situ early sedimentary diagenesis. Geochimica et Cosmochimica Acta 71:2344-2360

Li L, Bebout GE (2005) Carbon and nitrogen geochemistry of sediments in the Central American convergent margin: Insights regarding subduction input fluxes, diagenesis and paleoproductivity. Journal of Geophysical Research 110, B11202, doi:10.1029/2004JB003276

Li L, Bebout AE, Idleman BD (2007) Nitrogen concentration and $\delta^{15}N$ of altered oceanic crust obtained on ODP Legs 129 and 185: Insights into alteration-related nitrogen enrichment and the nitrogen subduction budget. Geochimica et Cosmochimica Acta 71:2344-2360

López Sánchez-Vizcaíno V, Gómez-Pugnaire MT, Garrido CJ, Padrón-Navarta JA, Mellini M (2009) Breakdown mechanisms of titanclinohumite in antigorite serpentinite (Cerro del Almirez massif, S. Spain): A petrological and TEM study. Lithos 107:216-226

López Sánchez-Vizcaíno V, Trommsdorff V, Gómez-Pugnaire MT, Garrido CJ, Müntener O, Connolly JAD (2005) Petrology of titanian clinohumite and olivine at the high-pressure breakdown of antigorite serpentinite to chlorite harzburgite (Almirez Massif, S. Spain). Contributions to Mineralogy and Petrology 149:627-646

Marroni M, Molli G, Montanini A, Tribuzio R (1998) The association of continental crust rocks with ophiolites in the Northern Apennines (Italy): implications for the continent-ocean transition in the Western Tethys. Tectonophysics 292:43-66

Marroni M, Pandolfi L (2007) The architecture of an incipient oceanic basin: a tentative reconstruction of the Jurassic Liguria-Piemonte basin along the Northern Apennines-Alpine Corsica transect. International Journal of Earth Sciences 96:1059-1078

Marty B, Dauphas N (2003) The nitrogen record of crust-mantle interaction and mantle convection from Archean to Present. Earth and Planetary Science Letters 206:397-410

Marty B, Humbert F (1997) Nitrogen and argon isotopes in oceanic basalts. Earth and Planetary Science Letters 152:101-112

Marty B, Zimmermann L (1999) Volatiles (He, C, N, Ar) in mid-ocean ridge basalts: Assessment of shallow-level fractionation and characterization of source composition. Geochimica et Cosmochimica Acta 63:3619-3633

Messiga B, Scambelluri M, Piccardo GB (1995) Formation and breakdown of chloritoid-omphacite high-pressure assemblages in mafic systems: evidence from the Erro-Tobbio eclogitic metagabbros (Ligurian Western Alps). European Journal of Mineralogy 7:1149-1167

Minoura K, Hoshino K, Nakamura T, Wada E (1997) Late Pleistocene-Holocene paleoproductivity circulation in the Japan Sea: Sea-level control on $\delta^{13}C$ and $\delta^{15}N$

records of sediment organic material. Paleogeography Paleoclimatology Paleoecology 135:41-50

Mitchell EC, Fischer TP, Hilton DR, Hauri EH, Shaw AM, de Moor JM, Sharp ZD, Kazahaya K (2010) Nitrogen sources and recycling at subduction zones: Insights from the Izu-Bonin-Mariana arc. Geochemistry Geophysics Geosystems 11: Q02X11, doi:10.1029/2009GC002783

Montanini A, Tribuzio R, Anczkiewicz R (2006) Exhumation history of a garnet pyroxenite-bearing mantle section from a continent-ocean transition (Northern Apennine Ophiolites, Italy). Journal of Petrology 47:1943-1971

Padrón-Navarta JA, Hermann J, Garrido CJ, López Sánchez-Vizcaíno V, Gómez-Pugnaire MT (2010) An experimental investigation of antigorite dehydration in natural silica-enriched serpentinite. Contributions to Mineralogy and Petrology 159:25-42

Padrón-Navarta JA, López Sánchez-Vizcaíno V, Garrido CJ, Gómez-Pugnaire MT (2011) Metamorphic record of high-pressure dehydration of antigorite serpentinite to chlorite harzburgite in a subduction setting (Cerro del Almirez, Nevado-Filábride Complex, Southern Spain). Journal of Petrology 52:2047-2078

Peters KE, Sweeney RE, Kaplan IR (1978) Correlation of carbon and nitrogen stable isotope ratios in sedimentary organic matter. Limnology and Oceanography 23:598-604

Philippot P, Busigny V, Scambelluri M, Cartigny P (2007) Oxygen and nitrogen isotopes as tracers of fluid activities in serpentinites and metasediments during subduction. Mineralogy and Petrology 91:11-24

Piccardo GB, Vissers RLM (2007) The pre-oceanic evolution of the Erro-Tobbio peridotite (Voltri Massif, Ligurian Alps, Italy). Journal of Geodynamics 43:417-449

Pitcairn IK, Teagle DAH, Kerrich R, Craw D, Brewer TS (2005) The behavior of nitrogen and nitrogen isotopes during metamorphism and mineralization: Evidence from the Otago and Alpine Schists, New Zealand. Earth and Planetary Science Letters 233:229-246

Puga E, Nieto JM, Díaz de Federico A, Bodinier J-L, Morten L (1999) Petrology and metamorphic evolution of ultramafic rocks and dolerite dykes of the Betic Ophiolitic Association (Mulhacén complex, SE Spain): Evidence of eo-Alpine subduction following an ocean-floor metasomatic process. Lithos 49:23-56

Rampone E, Hoffmann AW, Piccardo GB, Vannucci R, Bottazzi P, Ottolini L (1995) Petrology, mineral and isotope geochemistry of the External Liguride peridotites (northern Apennine, Italy). Journal of Petrology 36:81-105

Ranero CR, Phipps Morgan J, McIntosh K, Reichert C (2003) Bending-related faulting and mantle serpentinization at the Middle American trench. Nature 425:367-373

Rüpke LH, Phipps Morgan J, Hort M, Connolly, JAD (2004) Serpentine and the subduction zone water cycle. Earth and Planetary Science Letters 223:17-34

Sadofsky SJ, Bebout GE (2003) Record of forearc devolatilization in low-T, high-P/T metasedimentary suites: Significance for models of convergent margin chemical cycling. Geochemistry Geophysics Geosystems 4: 9003, doi:10.1029/2002GC000412

Sadofsky SJ, Bebout GE (2004) Nitrogen geochemistry of subducting sediments: New results from the Izu-Bonin-Mariana margin and insights regarding global nitrogen subduction. Geochemistry Geophysics Geosystems 5: Q03I15, doi:10.1029/2003GC000543

Sano Y, Takahata N, Nishio Y, Fischer TP, Williams S (2001) Volcanic flux of nitrogen from the Earth. Chemical Geology 171:263-271

Savov IP, Ryan JG, D'Antonio M, Fryer P (2007) Shallow slab fluid release across and along the Mariana arc-basin system: Insights from geochemistry of serpentinized peridotites from the Mariana fore arc. Journal of Geophysical Research 111, B09205, doi:10.1029/2006JB004749

Savov IP, Ryan JG, D'Antonio M, Kelley K, Mattie P (2005) Geochemistry of serpentinized peridotites from the Mariana Forearc Conical Seamount, ODP Leg 125: Implications for the elemental recycling at subduction zones. Geochemistry Geophysics Geosystems 6: Q04J15, doi:10.1029/2004GC000777.

Scambelluri M, Bottazzi P, Trommsdorff V, Vannucci R, Hermann J, Gómez-Pugnaire MT, López-Sánchez Vizcaíno V (2001) Incompatible element-rich fluids released by antigorite breakdown in deeply subducted mantle. Earth and Planetary Science Letters 192:457-470

Scambelluri M, Fiebig J, Malaspina N, Müntener O, Pettke T (2004) Serpentinite subduction: implications for fluid processes and trace-element recycling. International Geology Review 46:593-613

Scambelluri M, Piccardo GB, Philippot P, Robbiano A, Negretti L (1997) High salinity fluid inclusions formed from recycled seawater in deeply subducted alpine serpentinite. Earth and Planetary Science Letters 148:485-499

Scambelluri M, Tonarini S (2011) Subducted serpentinites are the boron reservoirs for arc magmatism. Goldschmidt Conference Abstracts, Mineralogical Magazine 75: 1806.

Sharp ZD, Barnes JD (2004) Water soluble chlorides in massive seafloor serpentinites: a source of chloride in subduction zones. Earth and Planetary Science Letters 226:243-254

Snyder G, Poreda R, Fehn U, Hunt A (2003) Sources of nitrogen and methane in Central American geothermal settings: Noble gas and ^{129}I evidence for crustal and magmatic volatile components. Geochemistry Geophysics Geosystems 4: 9001, doi:9010.1029/2002GC000363

Straub SM, Layne GD (2003) Decoupling of fluids and fluid-mobile elements during shallow subduction: Evidence from halogen-rich andesite melt inclusions from the Izu arc volcanic front. Geochemistry, Geophysics, and Geosystems 4: 9003, doi:10.1029/2002GC000349

Tatsumi Y, Kogiso T (1997) Trace element transport during dehydration processes in the subducted oceanic crust: 2. Origin of chemical and physical characteristics in arc magmatism. Earth and Planetary Science Letters 148: 207-221

Tolstikhin IN, Marty B (1998) The evolution of terrestrial volatiles: a view from helium, neon, argon and nitrogen isotope modelling. Chemical Geology 147:27-52

Tonarini S, Agostini S, Doglioni C, Innocenti F, Manetti P (2007) Evidence for serpentinite fluid in convergent margin systems: The example of El Salvador (Central America) arc lavas. Geochemistry, Geophysics, and Geosystems 8(9), doi:10.1029/2006GC001508

Ulmer P, Trommsdorff V (1995) Serpentine stability to mantle depths and subduction-related magmatism. Science 268:858-861

Trommsdorff V, López Sánchez-Vizcaíno V, Gómez-Pugnaire MT, Müntener O (1998) High pressure breakdown of antigorite to spinifex-textured olivine and orthopyroxene, SE Spain. Contributions to Mineralogy and Petrology 132:139-148

van der Straaten F, Schenk V, John T, Gao J (2008) Blueschist-facies rehydration of eclogites (Tian Shan, NW-China): implications for fluid-rock interaction in the subduction channel. Chemical Geology 225:195-219

Watenphul A, Wunder B, Heinrich W (2009) High-pressure ammonium-bearing silicates: Implications for nitrogen and hydrogen storage in the Earth's mantle. American Mineralogist 94:283-292

Yokochi R, Marty B, Chazot G, Burnard P (2009) Nitrogen in peridotite xenoliths: Lithophile behavior and magmatic isotope fractionation. Geochimica et Cosmochimica Acta 73:4843-4861

Figure captions:

Fig. 1: Pressure-temperature diagram showing the metamorphic evolution of oceanic mantle during subduction and some important dehydration reactions (modified from Scambelluri et al., 2004 and Padrón-Navarta et al., 2010). The arrow delineates the transition from oceanic serpentinites at low grades via high-pressure serpentinites to metamorphic chlorite peridotites at elevated P-T conditions.

Fig. 2: Plot of $\delta^{15}N_{air}$ values and N concentrations in ultramafic rocks. The field for the depleted mantle is from Marty and Dauphas (2003). Arrows indicate data points that plot outside the diagram limits. Abbreviations: LG serp. = low-grade serpentinite, HP serp. = high-pressure serpentinite, chl. hzbg. = chlorite harzburgite. Data for Raspas (Ecuador) and Cabo Ortegal (Spain) serpentinites from Halama et al. (2010). Data from Philippot et al. (2007) for peridotites from the South-West Indian Ridge (SWIR) and for peridotites and serpentinites from Erro Tobbio (ET-P07) are shown for comparison.

Fig. 3: Nitrogen concentrations and isotopic compositions of ultramafic rocks plotted against loss on ignition (LOI) as a measure of dehydration (symbols as in Fig. 2). The arrow indicates a data point that plots outside the diagram limits. Note that the chlorite harzburgites have consistently lower LOI values, but [N] and $\delta^{15}N_{air}$ are indistinguishable from high-pressure serpentinites. Dashed lines connect host serpentinite – vein pairs from Erro Tobbio.

Fig. 4: Frequency distribution diagrams of $\delta^{15}N_{air}$ values for low-grade serpentinites, high-pressure peridotites and high-pressure ultramafic veins. Data for HP serpentinites include analyses from the Raspas Complex (n=3) and from Cabo Ortegal (n=2) by Halama et al. (2010). DM = Depleted MORB source mantle from Marty and Dauphas (2003). Note the predominance of positive $\delta^{15}N_{air}$ values and the overlap between HP serpentinites, chlorite harzburgites and HP veins.

Fig. 5: Frequency distribution diagrams of $\delta^{15}N_{air}$ values for oceanic rocks (marine sediments and basaltic oceanic crust) and their respective subduction zone metamorphosed equivalents (metasediments and eclogites/blueschists representing metamorphosed oceanic crust). For data sources, see Table 2.

Fig. 6: Summary of the N budget calculations (Table 3) for the incoming plate consisting of marine sediments, igneous crust and serpentinized ultramafic rocks. Numbers in the pie diagrams give the contributions (in %) of the lithological units to the total N budget in the slab. Model slab sections used are depicted below.

Fig. 1

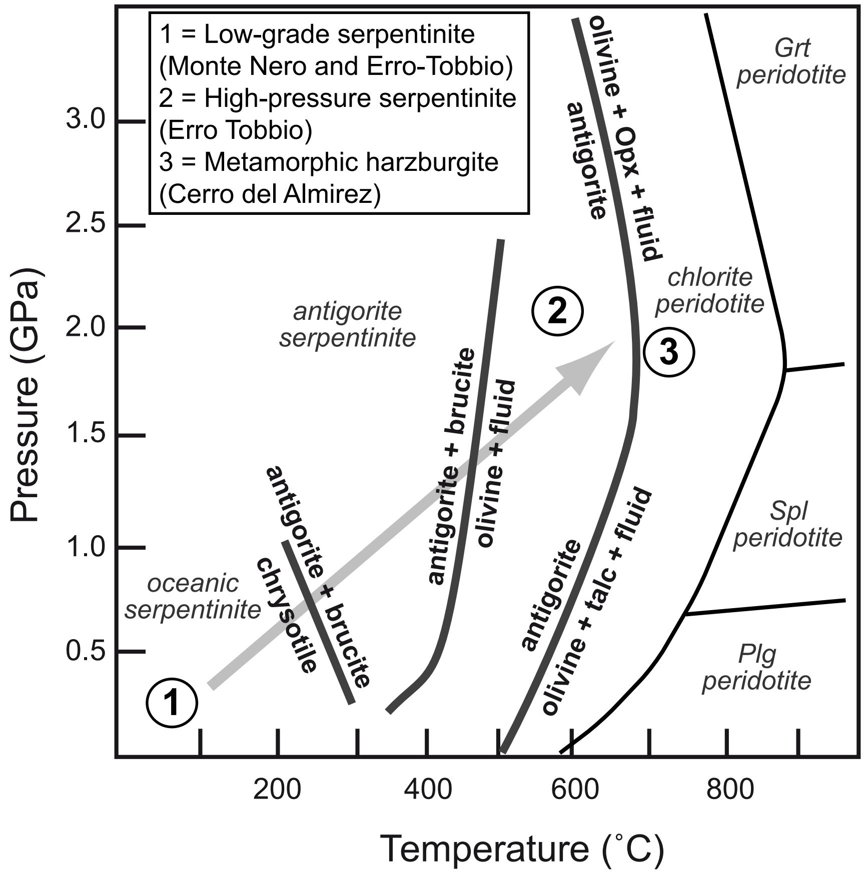

1 = Low-grade serpentinite
(Monte Nero and Erro-Tobbio)
2 = High-pressure serpentinite
(Erro Tobbio)
3 = Metamorphic harzburgite
(Cerro del Almirez)
Pressure (GPa)
Temperature (˚C)
3.0
2.5
2.0
1.5
1.0
0.5
200
400
600
800
antigorite serpentinite
oceanic serpentinite
antigorite + brucite
chrysotile
antigorite + brucite
olivine + fluid
antigorite
olivine + Opx + fluid
antigorite
olivine + talc + fluid
Grt peridotite
chlorite peridotite
Spl peridotite
Plg peridotite
1
2
3

Fig. 2

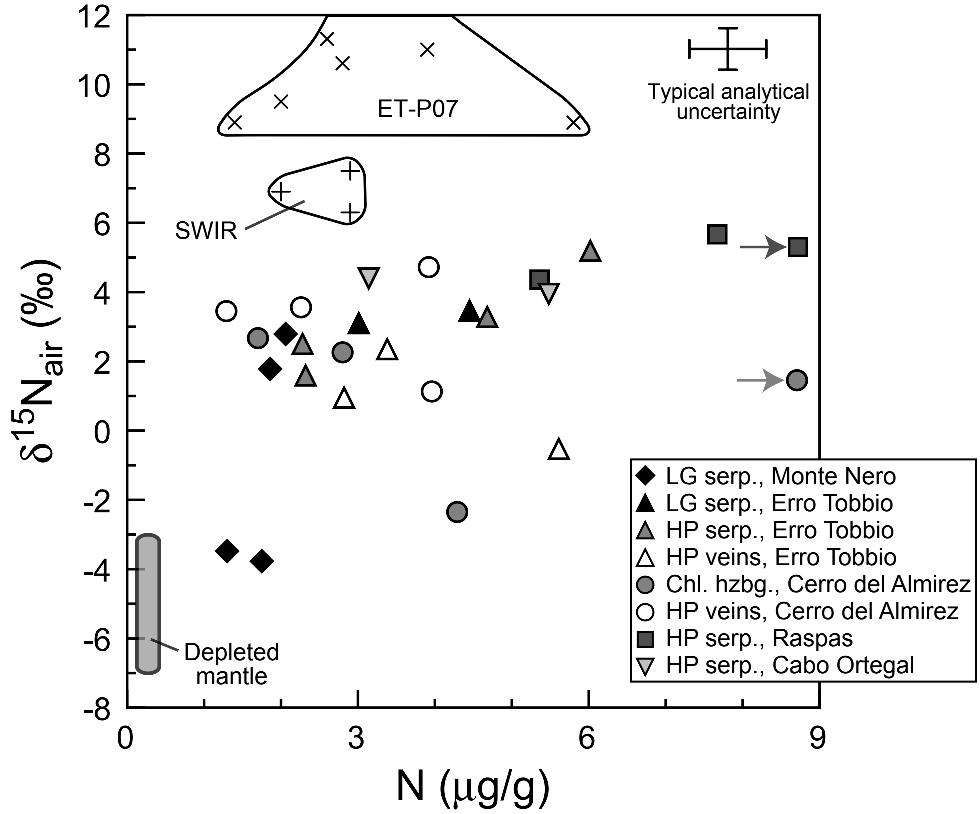

ET-P07
SWIR
Typical analytical uncertainty
Depleted mantle
$\delta^{15}N_{air}$ (‰)
N (µg/g)
12
10
8
6
4
2
0
-2
-4
-6
-8
0
3
6
9
LG serp., Monte Nero
LG serp., Erro Tobbio
HP serp., Erro Tobbio
HP veins, Erro Tobbio
Chl. hzbg., Cerro del Almirez
HP veins, Cerro del Almirez
HP serp., Raspas
HP serp., Cabo Ortegal

Fig. 3

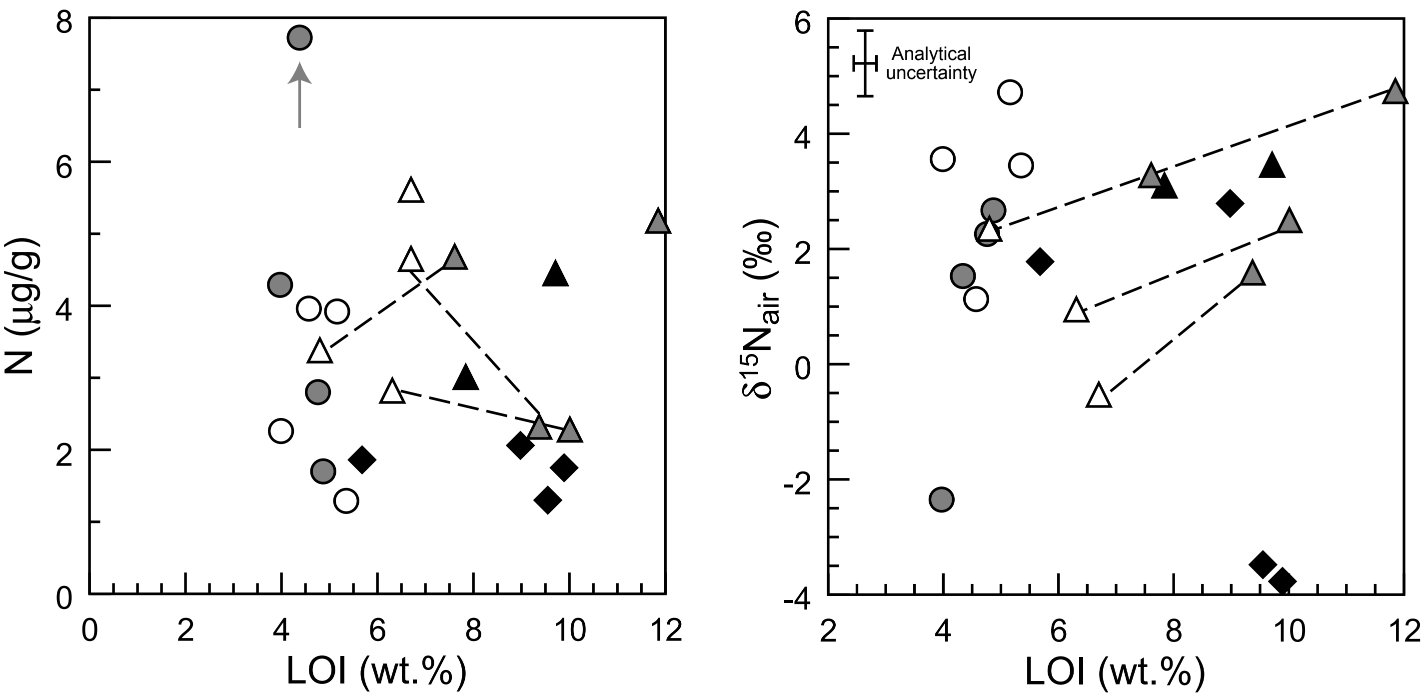

Fig. 4

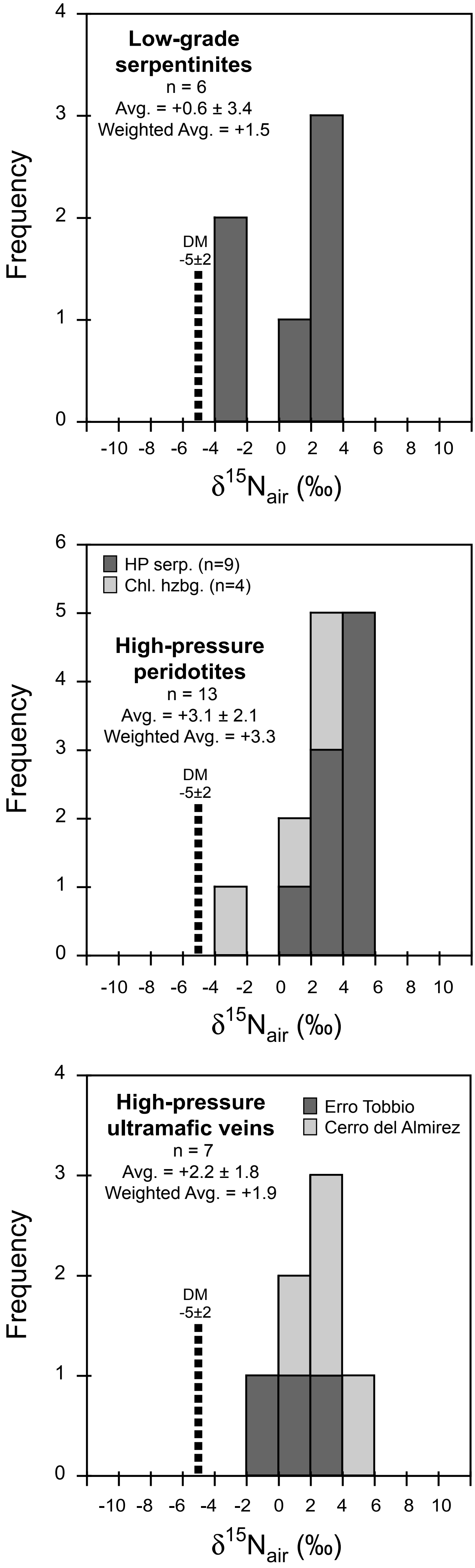
Low-grade serpentinites
n = 6
Avg. = +0.6 ± 3.4
Weighted Avg. = +1.5
DM
-5±2
Frequency
0
1
2
3
4
-10 -8 -6 -4 -2 0 2 4 6 8 10
δ15Nair (‰)
HP serp. (n=9)
Chl. hzbg. (n=4)
High-pressure peridotites
n = 13
Avg. = +3.1 ± 2.1
Weighted Avg. = +3.3
DM
-5±2
Frequency
0
1
2
3
4
5
6
-10 -8 -6 -4 -2 0 2 4 6 8 10
δ15Nair (‰)
High-pressure ultramafic veins
n = 7
Avg. = +2.2 ± 1.8
Weighted Avg. = +1.9
Erro Tobbio
Cerro del Almirez
DM
-5±2
Frequency
0
1
2
3
4
-10 -8 -6 -4 -2 0 2 4 6 8 10
δ15Nair (‰)

Fig. 5

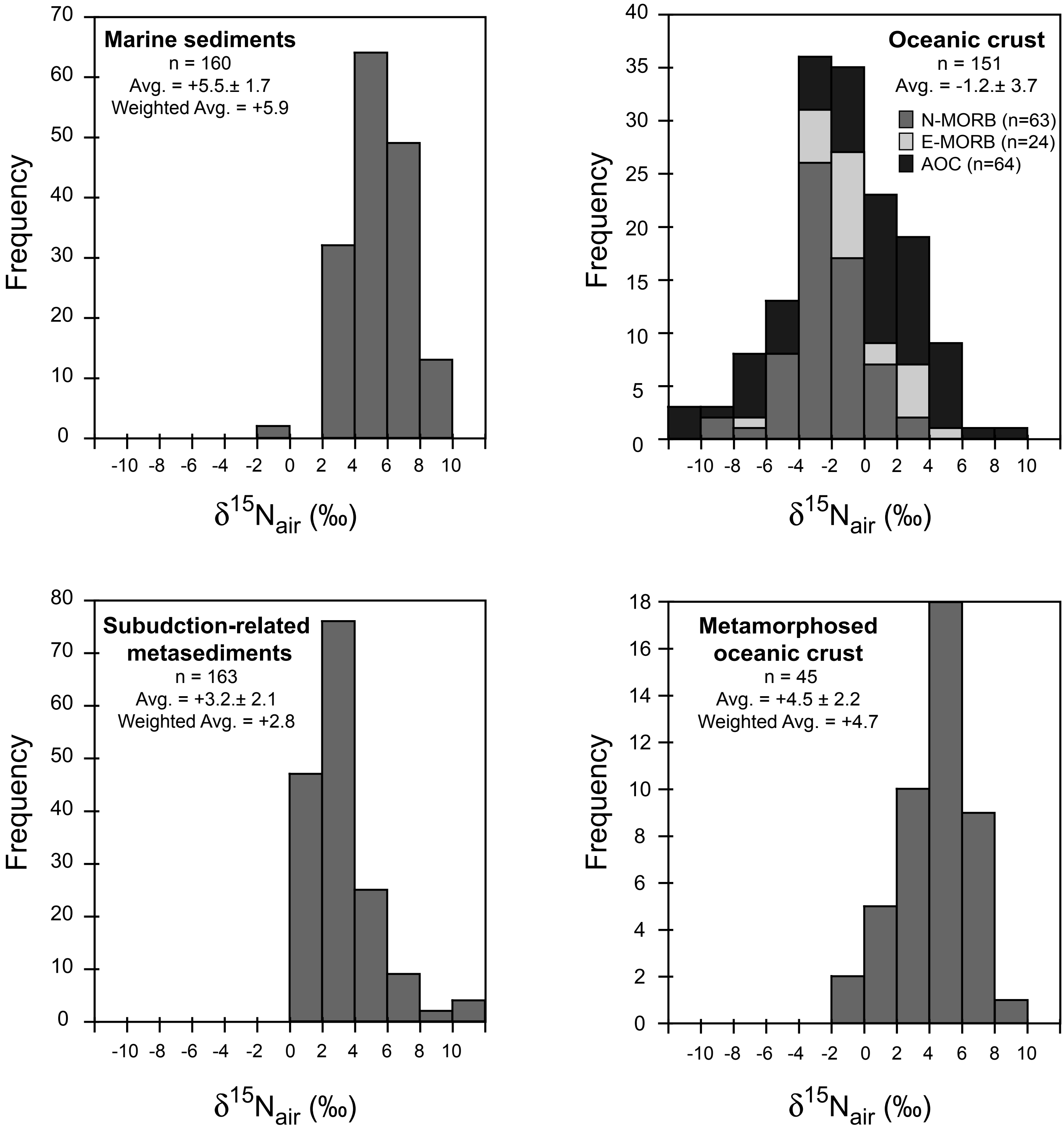
Marine sediments
n = 160
Avg. = +5.5.± 1.7
Weighted Avg. = +5.9
Frequency
δ15Nair (‰)
Oceanic crust
n = 151
Avg. = -1.2.± 3.7
N-MORB (n=63)
E-MORB (n=24)
AOC (n=64)
Subudction-related metasediments
n = 163
Avg. = +3.2.± 2.1
Weighted Avg. = +2.8
Metamorphosed oceanic crust
n = 45
Avg. = +4.5 ± 2.2
Weighted Avg. = +4.7

Table 1: Nitrogen concentrations and isotope compositions of ultramafic rocks

Sample #	Location	Rock type	Analysis #	[N] (µg/g)	$\delta^{15}N_{air}$ (‰)
MNS-1	Monte Nero	Low-grade serpentinite	1	2.06	2.79
MNS-2	Monte Nero	Low-grade serpentinite	1	1.75	-3.77
MNS-3	Monte Nero	Low-grade serpentinite	1	1.30	-3.48
MNS-4	Monte Nero	Low-grade serpentinite	1	1.86	1.78
ET Cl-2	Erro Tobbio	Low-grade serpentinite	1	3.01	3.33
			2	2.45	2.87
			AVG	2.73	3.10
ET Cl-3	Erro Tobbio	Low-grade serpentinite	1	4.45	3.46
Weighted average (n=6) low-grade serpentinites					**1.5**
ET Cl-4-1b-I	Erro Tobbio	HP serpentinite	1	6.02	5.19
			2	4.33	4.28
			AVG	5.18	4.74
ET Cl-7-1b-I	Erro Tobbio	HP serpentinite	1	2.28	2.50
ET Cl-7-4-I	Erro Tobbio	HP serpentinite	1	4.68	3.28
ET Cl-7-6-I	Erro Tobbio	HP serpentinite	1	0.54	
ET Cl-7-6-II	Erro Tobbio	HP serpentinite	1	2.32	1.59
Weighted average (n=4) HP serpentinites (Erro Tobbio)					**3.4**
ET Cl-4-1b-v	Erro Tobbio	HP vein	1	3.38	2.35
ET Cl-7-1b-v	Erro Tobbio	HP vein	1	2.82	0.95
ET Cl-7-6-v	Erro Tobbio	HP vein	1	5.61	-0.53
Weighted average (n=3) HP veins (Erro Tobbio)					**0.6**
ALM-1	Almirez	Chlorite harzburgite	1	4.29	-2.35
ALM-6	Almirez	Chlorite harzburgite	1	1.70	2.67
ALM-8	Almirez	Chlorite harzburgite	1	2.80	2.26
ALM-95-64	Almirez	Chlorite harzburgite	1	20.3	1.58
			2	20.9	1.48
			AVG	20.6	1.53
Weighted average (n=4) chlorite harzburgites (Almirez)					**1.1**
ALM-11	Almirez	HP vein	1	3.92	4.72
ALM-11v	Almirez	HP vein	1	1.29	3.45
ALM-13v	Almirez	HP vein	1	3.96	1.13
ALM-13/3v	Almirez	HP vein	1	2.26	3.56
Weighted average (n=4) HP veins (Almirez)					**3.1**

Table 2: Compilation of nitrogen concentrations and $\delta^{15}N$ data of slab lithologies and their metamorphosed equivalents

	n	AVG [N]	STDEV [N]	Median [N]	AVG $\delta^{15}N_{air}$	STDEV $\delta^{15}N_{air}$	Weighted AVG $\delta^{15}N_{air}$	Reference
		µg/g	µg/g	µg/g	‰	‰	‰	
Marine sediments								
Northwest Pacific, Izu-Bonin arc	36	286	142	312	4.7	1.7	5.0	Sadofsky & Bebout 2004
East Pacific, west off Costa Rica	65	771	682	699	5.5	1.5	6.2	Li & Bebout 2005
Northeast Pacific	55				6.1	1.8		Peters et al. 1978
Unmetamorphosed sediments, Western Alps	4	416	251	338	3.9	0.7	4.0	Busigny et al. 2003
Subduction-related metasediments								
Western Alps, Schistes Lustrés	12	643	545	485	3.5	0.7	3.4	Busigny et al. 2003
Western Baja Terrane	5	390	183	305	1.8	1.0	2.0	Sadofsky & Bebout 2003
Franciscan Complex	27	420	283	385	1.7	0.8	1.9	Sadofsky & Bebout 2003
Franciscan Complex	44	405	298	325	2.5	1.2	2.3	Bebout & Fogel 1992
Raspas Complex, Ecuador	3	123	98	143	3.8	0.8	4.2	Halama et al. 2010
Erzgebirge, European Variscan Belt	58	243	204	195	4.5	2.6	3.6	Mingram & Bräuer 2001
Otago and Alpine Schist, New Zealand	15	296	136	369	3.5	1.3	3.7	Pitcairn et al. 2005
Oceanic lithosphere								
N-MORB	63				-2.3	2.3		MZ1999, MH1997, C2001
E-MORB (includes T- and P-MORB)	24				-0.4	2.6		MZ1999, MH1997, C2001
AOC, Site 1256, Pacific	15	2.8	0.8	3.0	3.9	1.2	3.9	Busigny et al., 2005
AOC, Site 801	26	6.9	5.4	4.3	-2.5	4.0	-0.7	Li et al., 2007
AOC, Site 1149	9	2.0	0.5	2.1	-5.2	3.1	-5.0	Li et al., 2007
AOC, North Atlantic	5	11.4	2.5	11.9	2.5	5.2	2.9	Li et al., 2007
AOC, Philippine Sea	2	9.1	3.7	9.1	3.6	0.4	3.6	Li et al., 2007
AOC, Antarctic	2	4.0	1.0	4.0	2.4	2.6	2.7	Li et al., 2007
Low-grade serpentinites	6	2.4	1.1	2.0	0.6	3.4	1.5	This study
Metamorphosed oceanic lithosphere								
Undeformed and low-strain metagabbros	8	9.4	8.3	6.4	5.0	2.3	3.8	Busigny et al., 2011
Mylonites and veins, Western Alps	7	18.3	17.2	15.9	2.9	1.8	3.2	Busigny et al., 2011
Blueschists	3	24.5	19.0	14.0	5.7	1.7	6.4	Halama et al., 2010
MORB-type eclogites	25	6.0	3.8	4.9	4.1	1.9	4.0	Halama et al., 2010
Metasomatic eclogites	9	5.4	2.8	4.9	4.5	3.1	5.4	Halama et al., 2010
High-pressure peridotites, Ecuador and Spain	5	7.3	4.5	5.5	4.8	0.8	5.1	Halama et al., 2010
High-pressure peridotites, Western Alps/Italy	5	3.0	1.9	2.3	3.0	1.3	3.4	This study
High-pressure ultramafic veins, Western Alps/Italy	3	3.9	1.5	3.4	0.9	1.4	0.6	This study
Chlorite harzburgites, Betic Cordillera/Spain	4	7.4	8.9	3.6	1.0	2.3	1.1	This study
High-pressure ultramafic veins, Betic Cordillera/Spai	4	2.9	1.3	3.1	3.2	1.5	3.1	This study

MZ1999 = Marty and Zimmermann, 1999; MH1997 = Marty and Humbert, 1997; C2001 = Cartigny et al., 2001

Table 3: Calculations for the flux of subducted nitrogen and its isotopic composition

	Thickness	Density	[N]	Flux	Flux	$\delta^{15}N_{air}$	Flux contribution	Data source
	m	$g/m^3 \times 10^6$	$g/g \times 10^{-6}$	$g/year \times 10^9$	$mol/year \times 10^9$	‰	%	
Sediment	500	2.00	286	629	22.5	5.0		Sadofsky and Bebout, 2004
Sediment	500	2.00	771	1696	60.6	6.2		Li and Bebout, 2005
AOC	6000	2.89	2.80	107	3.81	3.9		Busigny et al., 2005
AOC	6000	2.89	6.90	263	9.40	-0.7		Li et al., 2007
AOC	6000	2.89	11.4	435	15.5	2.9		Li et al., 2007
Serpentinized mantle	500	2.90	1.80	5.74	0.205	-0.3		This study, MNS samples only
Serpentinized mantle	500	2.90	2.40	7.66	0.273	1.5		This study, all oceanic peridotites
Unmetamorphosed slab section:								
Case A								
Sediment	500	2.00	365	803	28.7	5.9	86	
AOC	6000	2.89	3.30	126	4.50	-1.2	13	
Serpentinized mantle	500	2.90	2.00	6.38	0.228	1.5	1	
Total				935	33.4	4.9	100	
Case B: Reduced sediment thickness								
Sediment	100	2.00	365	161	5.74	5.9	55	
AOC	6000	2.89	3.30	126	4.50	-1.2	43	
Serpentinized mantle	500	2.90	2.00	6.38	0.228	1.5	2	
Total				293	10.5	2.8	100	
Case C: Increased serpentinization depth								
Sediment	500	2.00	365	803	28.7	5.9	76.0	
AOC	6000	2.89	3.30	126	4.50	-1.2	11.9	
Serpentinized mantle	10000	2.90	2.00	128	4.56	1.5	12.1	
Total				1057		4.5	100	
Metamorphosed slab section:								
Case A								
Metasediment	500	2.70	287	852	30.4	2.8	77.3	
Met. Oceanic crust	6000	3.50	5.10	236	8.42	4.7	21.4	
Met. Serpentinized mantle	500	3.00	4.50	14.9	0.530	3.3	1.3	
Total				1103	39.4	3.2	100	
Case B: Reduced sediment thickness								
Metasediment	100	2.70	287	170	6.09	2.8	40.5	
Met. Oceanic crust	6000	3.50	5.10	236	8.42	4.7	56.0	
Met. Serpentinized mantle	500	3.00	4.50	14.9	0.530	3.3	3.5	
Total				421	15.0	3.9	100	
Case C: Increased serpentinization depth								
Sediment	500	2.70	287	852	30.4	2.8	61.5	
AOC	6000	3.50	5.10	236	8.42	4.7	17.0	
Serpentinized mantle	10000	3.00	4.50	297	10.6	3.3	21.4	
Total				1385		3.2	100	

The calculations assume a convergence rate of 0.05 m/year and a total arc length of 44000 km (Straub and Layne, 2003)
Densities for the metamorphosed lithological components are based on data for metamorphosed MORB and harzburgite at 600°C and 25 kbar (Hacker et al., 2003)
The N concentrations given for the bulk slab calculations reflect median values.